Mission-Driven Resource Management for Reconfigurable Sensing Systems

de Groot, Teun H.; Krasnov, Oleg A.; Yarovyi, Alexander G.

DOI
10.1109/JSYST.2016.2599072

Publication date
2018

Document Version
Final published version

Published in
IEEE Systems Journal

Mission-Driven Resource Management for Reconfigurable Sensing Systems

Teun H. de Groot, Oleg A. Krasnov, and Alexander G. Yarovoy, *Fellow, IEEE*

***Abstract*—Modern sensors, such as multifunctional radars, comprise many settings and the number of controllable settings is increasing due to technological advance. Although having many settings allows many capabilities, it simultaneously requires an automatic manager to control them. This paper proposes mission-driven resource management to control reconfigurable sensing systems during run time. It works as follows. First, expected mission success is defined from an end-user point of view. Because such criterion can eventually be mathematically linked to the adaptable parameters of the reconfigurable systems, these parameters can be optimally selected. To illustrate, a case study is considered where many heterogeneous high-level operational tasks (i.e., air defense, weather alarm, crowd control, and drone flight) have to be supported by several fully reconfigurable radio-frequency antenna front ends. This paper analytically and numerically compares the proposed mission-driven method that maximizes end-user's expectations for mission success, with a traditional task-driven one, that solely optimizes task performance characteristics. To conclude, by maximizing expected mission success, the systems are automatically adapted to new circumstances, and the end-user's mission is constantly supported by the system in the most effective way.**

***Index Terms*—Mission success, optimal control, reconfigurable architectures, resource management, utility theory.**

I. Introduction

THE management of modern multifunctional and reconfigurable sensors is in practice too complex for end users, because there are too many choices for humans to consider and they are too strongly related to advanced aspects of sensor technology. Furthermore, the changes in environment, threats and systems can happen too fast for an end user to react to. Thus, utilizing these sensors at their full capability requires automatic *resource management*.

A. Previous Work

A management solution can be based on *heuristics*, which refers to methods based on lookup tables, if–then programs, fuzzy logic, and rules of thumb (e.g., [1]–[3]). Heuristics can be very fast—and even optimal—for a limited set of problems, but the key disadvantage is that it is too hard to theoretical validate their optimality, especially when changes in the operational conditions and scenarios are expected.

Manuscript received July 7, 2015; revised June 1, 2016; accepted July 19, 2016. Date of publication September 5, 2016; date of current version May 2, 2018. This work was supported by the Sensor Technology Applied in Reconfigurable Systems (STARS) project funded by the Dutch Government.

The authors are with Microwave Sensing, Signals and Systems, Delft University of Technology, 2628 CD Delft, The Netherlands (e-mail: T.H.deGroot@tudelft.nl; O.A.Krasnov@tudelft.nl; A.Yarovoy@tudelft.nl).

Digital Object Identifier 10.1109/JSYST.2016.2599072

A better optimization method is based on an *objective function*. Such an objective function then quantifies performance with an ordinal (or cardinal) number, and allows to unambiguously compare optimality of solutions. In this way, the optimization goal is mathematically clear and the algorithm is more robust against changing situations and scenarios.

Many objective functions have been proposed to measure task performance based on *technical characteristics*. Popular characteristics in sensor management are (cumulative) target detection probability (e.g., [4]–[6]), tracking accuracy (e.g., [7] and [8]), measures in the information theory (e.g., [8]–[11]), and signal power/energy (e.g., [12]–[15]) or other qualities (e.g., [16]–[19]). Similar metrics are used in the communication domain: packet/bit (error) rates (e.g., [20] and [21]), signal/power (interference) levels (e.g., [22]–[24]) or throughput/latency (e.g., [23] and [25]).

Some sensors are *multifunctional* and can simultaneously execute many tasks and adapt for each task the settings. The aforementioned metrics vary between task types (i.e., not comparable), but a decision has to be made to tradeoff between these task performances when there are limited resources and many tasks.

The *task-driven* approach deals with many tasks as follows. A single additive-utility function (e.g., [5], [7], [16]–[18], [26], and [27]) is used to combine all individual task performances. Such utility function is usually a summation of task -utilities or task- qualities multiplied with their priorities or weights. Threat assessment can sometimes used for task prioritization (e.g., [28]–[30]). There remain several issues. For instance, there exist no consistent meaning of utility, because the qualities are described with incompatible technical characteristics. Although the optimal allocation of tasks is claimed by maximizing such utility, there is no justification that the aforementioned utility definition equals the utility for the end-user's mission.

A *risk-driven* approach is based on cost or loss definitions and can have more operational meaning for end users [29], [31]. However, in several cases, resource characteristics are involved in its definition (e.g., risk of losing track [7], misclassification [32], and cost of weapon deployment [33]). This does not address the essential aspect of the mission, because the systems are actually not employed for the benefit of the resources themselves, but to achieve mission goals.

To conclude, the dominant idea is that optimization should be driven by sensing and system characteristics. In contrast, a *mission-driven* solution would just configure systems in such a way that they contribute as much as possible to the end-user's

mission. This concept gets only recently interest and little related works exist (e.g., [29] and [33]). We consider it very beneficial for end users and discussed the principles and some aspects of mission-driven objective functions [34], [35]. However, it is yet unclear how the performance compares from a mission point of view to a task-driven approach.

B. Presented Work

This paper's contribution is a resource manager that maximizes the end-user's expectations for mission success, instead of solely optimizing task performance characteristics, and compares it *analytically* and *numerically* in a dynamic security case study with a task-driven approach.

The mission-driven approach works as follows. First, expected mission success is defined. This metric depends on many aspects such as performance of sensors, effectors, data communication, and human operators. Second, the adaptable system parameters are mathematically linked to expected mission success. Finally, by maximizing expected mission success, the settings within tasks and tradeoffs between different types of tasks are automatically and optimally selected.

To illustrate, we consider a case study involving the security of a large event where many threats and related operational tasks are defined. The controllable systems are four fully reconfigurable radio-frequency (RF) antenna front ends, which allow to implement many design solutions and capabilities (e.g., radar surveillance and radio communication) during run time.

The structure of this paper is as follows. Section II proposes the mission-driven objective function and links it to an operational task metric. Section III analytically determines the improvement over a traditional task-driven method. Section IV defines a case study with several operational tasks for numerical comparison. A reconfigurable resource model is presented in Section V. In Section VI, it is demonstrated that the system can be automatically reconfigured, and compares the mission-driven method with traditional ones. Section VII concludes this study and summarizes the impact of the presented results. Appendices A–D present methods to estimate the quality of specific operational tasks execution.

II. Developed Mission-Driven Objective

This section proposes an objective function that combines all aspects important to the end users (e.g., prevent any damage, calamities, and/or panic). In addition, its relation to an operational task performance metric is determined.

A. Mission Success

The mission is defined successful if all goals are achieved at the moment that the mission is originally planned to end. In this case, the *utility* for the end user is maximized. This means that "mission success" can be quantified as follows:

$$U = \sum_{z=1}^{Z} u_z \tag{1}$$

where u_z is the utility of achieving goal z. Thus, when all goals are achieved after the mission, then utility U is maximized and the mission is a full success. To emphasize, this utility is not based on task execution, as in a traditional task-driven solution, but on obtained mission results.

The definition of the goal utility u_z is a challenging task. To make goals tangible, they can be related to obtaining or losing assets, which can be defined in various ways, as in Section IV. A suggestion can then be to determine its economic value (e.g., in euro currency). However, apart from conceptual differences in the definition of the economic value (e.g., cost of replacing it, cost of losing it, gain of selling it), it becomes very hard when humans are (part of) the goals/assets.

There remain also other possibilities to define utility values u_z. When an asset is the main tent during a large event, it can also be linked to the calmness of the people inside. If the calmness level remains high, then the asset is secured. If a calamity and/or panic occurs, the calmness level decreases and the asset is not secured. Another possibility is to measure utility in terms of reputation. End users have indicated that political impact of an accident is sometimes more important than actual physical impact. In this case, the utility could be related to the amount of negative attention in the media.

B. Mission Success Expectations

A fundamental problem is that goal utility u_z at the end of the mission cannot be determined before the mission has ended. In reality, it is unpredictable what will actually happen and which assets will be affected during the mission. As a result, value U is beyond the system's control. However, it is possible to maximize "mission success expectations" by employing the *expected-utility* model [36], [37]

$$U_E = \sum_{z=1}^{Z} u_z P(S_z) \tag{2}$$

where $P(S_z)$ is the probability that goal/asset z is secured (i.e., obtained by capturing and/or retained by protecting) when the mission ends. Note, maximization of U_E does not guarantee maximum U, but it maximizes its expectations for it.

Let us assume that threats exist that can prevent the end user from obtaining mission success. To counter these threats, operational tasks can be defined. The probability that an operational task k is successfully executed for goal z is then related to the expected utility, as expressed by following formula:

$$\begin{aligned} P(S_z) &= \prod_{k=1}^{K} P(S_{\mathrm{zk}}) \\ &= \prod_{k=1}^{K} \big(1 - P(E_k)(1 - P(S_{\mathrm{zk}}|E_k))\big) \end{aligned} \tag{3}$$

where $P(E_k)$ is the probability that the threat, that is described by operational task k, becomes reality. In the aforementioned definition, it is assumed that all threats can nullify the goal utility. Of course, an alternative solution that is less strict is also possible.

The probability that an operational task k is successfully executed in perspective of goal z is calculated by testing the system response during N_k possible scenarios

$$P(S_{\mathrm{zk}}|E_k) = \sum_{n=1}^{N_k} P(S_{\mathrm{zk}}|X_{kn})P(X_{kn}|E_k) = \mathrm{QoS}_{\mathrm{zk}} \quad (4)$$

where S_{zk} means that asset z is secured against the threatening event specified in operational task k, E_k means that the event specified in operational task k occurs during the mission, and X_{kn} is a possible scenario n within operational task k. A scenario is a detailed description of a possible incident (e.g., a small air object takes trajectory $n = 23$ toward asset $z = 2$) within a general event (e.g., an air object attacks).

The aforementioned analysis is very flexible and broad. A scenario is, for example, not limited to a single attacking object, but can consist of multiple threatening objects attacking an asset. Moreover, a single scenario, such as a weather storm, can damage multiple assets. It is also possible that scenarios of different types of operational tasks happen at the same time (e.g., an ultralight and agitated crowds).

The difficulties associated with finding the task performance probabilities should not be underestimated. Nevertheless, the appendices provide some possible techniques to find them. Although the exact performance evaluation method has no effect on the concept of management, it is important to understand that the correctness of the model output influences the practical optimality of model-based optimization.

The operational task performance is referred to as quality-of-service (QoS). This can be presented to the end user to express the impact of system performance on mission goals. Moreover, it allows to analytically compare a mission-driven method with a task-driven one, as conducted in Section III.

III. Improvement Over Task-Driven Objective

This section analytically investigates the improvement of directly maximizing mission success expectations instead of maximizing a task-driven objective.

A task-driven objective function is derived based on the discussed principle (e.g., [5], [7], [16]–[18], [26], and [27]) of multiplying task qualities with their priorities

$$U_Q = \sum_{z=1}^{Z}\sum_{k=1}^{K} p_{\mathrm{zk}}\mathrm{QoS}_{\mathrm{zk}} \quad (5)$$

where p_{zk} is the priority of asset-task combination zk. Let us assume that the priorities are based on a threat assessment approach (e.g., [3], [29], and [30]). The event's threat assessment is reused for this purpose

$$p_{\mathrm{zk}} = u_z P(E_k). \quad (6)$$

The theoretical boundaries of the improvement ratio are determined by analyzing the following two cases.

In the first case, there is only a single task for one asset. Thus, there is only one $\mathrm{QoS}_{\mathrm{zk}}$ that can be optimized. When $P(E_k)$ and u_z are nonzero, maximizing U_Q or U_E results in the same allocation in which $\mathrm{QoS}_{\mathrm{zk}}$ is maximized (there are no other $\mathrm{QoS}_{\mathrm{zk}}$ to spend resources on). Therefore, all solutions have the same mission success expectations, and the improvement of using the developed mission-driven objective instead of a task-driven objective is zero (i.e., ratio is one).

Let us assume in the second case two assets and three tasks. Task $k = 1, 2$ for asset $z = 1$ and task $k = 3$ for asset $z = 2$. The mission-driven method results in the following equation:

$$U_E = u_1\big(1 - P(E_1)(1 - \mathrm{QoS}_{11})\big)\big(1 - P(E_2)(1 - \mathrm{QoS}_{12})\big) + u_2\big(1 - P(E_3)(1 - \mathrm{QoS}_{23})\big). \quad (7)$$

The task-driven method results in following equation:

$$U_Q = u_1 P(E_1)\mathrm{QoS}_{11} + u_1 P(E_2)\mathrm{QoS}_{12} + u_2 P(E_3)\mathrm{QoS}_{23}. \quad (8)$$

When $P(E_1) = 1$ and $\mathrm{QoS}_{11} = 0$ in all cases (i.e., QoS_{11} cannot be changed by the resources), then losing asset $z = 1$ can be better accepted, and all resources should be devoted to at least save asset $z = 2$ (i.e., no resources should be spent on QoS_{12}). In other words, find the allocation that maximizes the mission success expectations

$$\begin{aligned}\mathbf{A_E} &= \arg\max_{\mathbf{A}}\{U_E\} \\ &= \arg\max_{\mathbf{A}}\big\{u_2\big(1 - P(E_3)(1 - \mathrm{QoS}_{23})\big)\big\} \\ &= \arg\max_{\mathbf{A}}\{\mathrm{QoS}_{23}\} \end{aligned} \quad (9)$$

where function arg retrieves the allocation $\mathbf{A}$ of the optimization max. Allocation $\mathbf{A}$ comprises all tunable parameters.

A task-driven additive-utility objective formulation does not optimize directly the impact for the mission. Therefore, it may remain spending resources on QoS_{12}

$$\mathbf{A_Q} = \arg\max_{\mathbf{A}}\{U_Q\} = \arg\max_{\mathbf{A}}\{u_1 P(E_2)\mathrm{QoS}_{12} + u_2 P(E_3)\mathrm{QoS}_{23}\}. \quad (10)$$

In the worst case (e.g., $u_1 P(E_2)$ is very high), the task-driven optimization spends all resources on QoS_{12} at the cost of QoS_{23}. As a result, $U_E(\mathbf{A_Q}) = 0$. The improvement of using the mission-driven objective instead of the task-driven one is then infinite (i.e., $U_E(\mathbf{A_E})$ divided by zero).

To conclude, the improvement ratio is within the range of $[1, \infty)$. Thus, the obtained performance cannot be worse, is at least equal, and potentially much better.

IV. Case Study

Assume that a large event, which has attracted the attention of many people, is organized as depicted in Fig. 1. In practice, the number of possible accidents during such events is unlimited, but the available resources to prevent them are scarce. In order to quantify the risks, the following four high-valued assets have been identified by the event's organizers:

1) the main tent and the people within it;
2) a mobile base station for public communication;
3) a moving very-important person (VIP);
4) a camera-equipped drone for crowd control.

As shown in Fig. 1, there are also effector units, which are deployed to intercept objects that pose a threat to the relevant

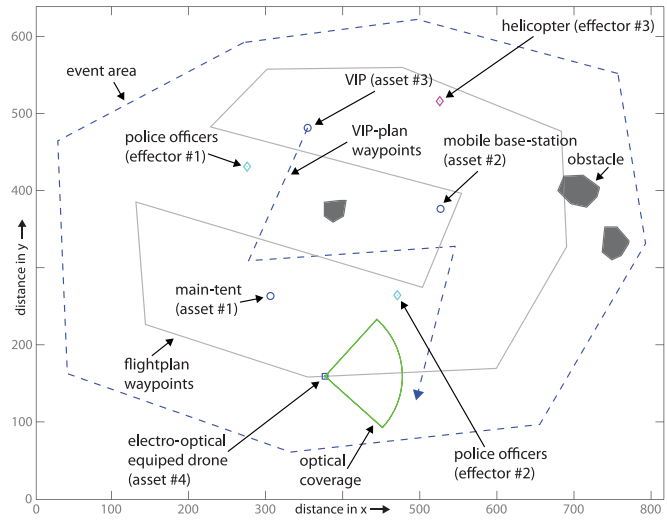

Fig. 1. Top view of the large event security study case.

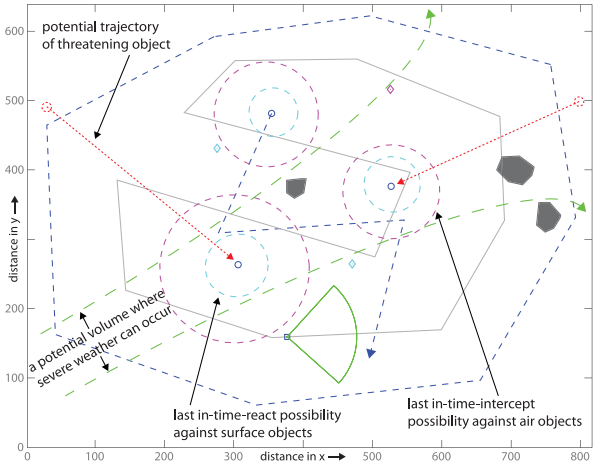

Fig. 2. Top view of large event security including threats.

assets. The first two effectors are surface units (e.g., police officers) and can intervene on the ground. The third one (e.g., helicopter) can fly and intercept small air units.

Another duty for the responsible security services of the event management is to assess future threatening scenarios. Solutions exist to support end users in threat assessment (e.g., [38]–[40]), but detailed discussions are considered beyond the scope of this paper. Assume that based on such a conducted assessment, following four types of threats are defined:

1) an unmanned ultralight can fly over the event and attack an asset;
2) a weather storm may approach, causing severe winds that may lead to calamities;
3) people in the crowd on location can start to form groups, get agitated, and maybe even behave aggressively;
4) the autopilot of the surveillance drone may fail, which is devastating to the event security.

The ultralight and storm threats are illustrated in Fig. 2. Based on the four threats, following four types of operational tasks are formulated:

1) air defense against potential flying threatening objects;

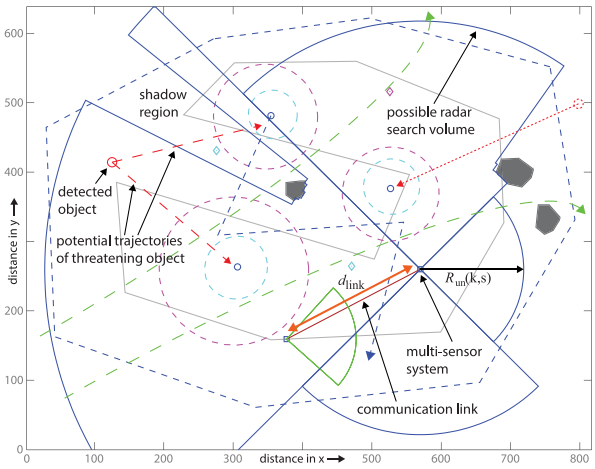

Fig. 3. Reconfigurable multisensor system deployed at the event, as discussed in Section IV. The figure additionally shows possible air surveillance coverages and communication link with the drone. $R_{\text{un}}(k,s)$ is the unambiguous and maximum range for operational task $k = 1, 2$ and sensor s. d_{link} is the distance between the multisensor system and drone.

2) weather observation/alarm for sudden severe storms;
3) crowd control against potential threatening groups;
4) drone control to correct instructions of autopilot.

The Appendices A, B, C, and D present methods to estimate task performance $P(S_{\text{zk}}|E_k)$. We are aware that some aspects are simplified and may not be well aligned for all cases with current practices of safety services. However, as explained in Section II, the exact performance evaluation method has no effect on the concept of model-based management.

V. Reconfigurable Resource Model

A platform is deployed within the fictional event as shown in Fig. 3. The platform is equipped with four reconfigurable RF front ends that are oriented to the North, East, South, and West. The RF front ends are identical, thus all four have the same model. This section presents radar surveillance, radio communication, and reconfigurable antenna front-ends models that connect the system characteristics to the operational task parameters.

A. Radar Surveillance

The radar surveillance capability is simultaneously needed for operational tasks $k = 1, 2$ (i.e., air defense and weather alarm). One of the possibilities of a reconfigurable RF front end is that it can be configured to provide an agile radar pencil beam that can search for objects in a specified volume. An example of search volumes for each of the RF front ends for air surveillance for operational task $k = 1$ is given in Fig. 3. The search volumes for each RF front end can be adjusted separately.

When the radar pencil beam is pointed to an object, then the single pulse signal-to-noise-ratio is given by [41], [42]

$$\text{SNR}_{\text{knm}} = \frac{P_S G_S^2 \lambda^2 \text{RCS}_{\text{knm}}}{(4\pi)^3 R_{\text{knm}}^4 N L} \tag{11}$$

where P_S is surveillance transmit power, G_S is surveillance antenna gain, λ is radar wavelength, RCS_{knm} is radar cross section of the expected object in scenario n defined by operational task type $k = 1, 2$ during measurement m, R_{knm} is the object range during measurement m, scenario n for operational task k, N is noise power, and L is system losses. Note, P_S, G_S, and RCS_{knm} have to correspond to the sensor that is executing measurement m during scenario n.

The radar detection probability $P_D(\text{SNR}, n_p, P_{\text{fa}})$ of a target with Swerling fluctuation depends on the single pulse SNR, the selected false alarm rate P_{fa} and the number of processed pulses n_p [41]. Thus, P_{knm} at moment m during scenario n for operational task $k = 1, 2$ is given by

$$P_{\text{knm}} = P_D(\text{SNR}_{\text{knm}}, n_k, P_{\text{fa}}(k)) \tag{12}$$

where n_{ks} is the selected number of transmitted pulses by sensor s for operational task $k = 1, 2$, and $P_{\text{fa}}(k)$ is the selected false alarm probability for air or weather surveillance.

The revisit time of sensor s in the search volume for operational task $k = 1, 2$ is estimated as

$$\text{RT}_{\text{ks}} = \frac{\text{DT}_{\text{ks}}}{a_{\text{ks}}} \left\lceil \frac{\theta_k}{\theta_s} \right\rceil \left\lceil \frac{\phi_k}{\phi_s} \right\rceil \tag{13}$$

where DT_{ks} is the dwell time for a single beam search position, a_{ks} specifies between range $[0, 1]$ the allocated time resources to task k, θ_s and ϕ_s are the radar beamwidths for a sensor s in azimuth and elevation, respectively, and θ_k and ϕ_k are the search volumes for operational task $k = 1, 2$ in azimuth and elevation, respectively. Operator $\lceil . \rceil$ is a ceiling function. For a high pulse repetition tnterval (PRI) radar, the dwell time for one beam position is given by

$$\text{DT}_{\text{ks}} = n_{\text{ks}} \text{PRI}_{\text{ks}} = n_{\text{ks}} \left(\frac{2R_{\text{un}}(k, s)}{c_w} + \tau_{\text{ks}} \right) \tag{14}$$

where n_{ks} is number of pulses, τ_{ks} is pulse length, $R_{\text{un}}(k, s)$ is unambiguous and maximum range for operational task $k = 1, 2$ and sensor s, and c_w is the wave propagation speed.

The radar range resolution ΔR and cross-range resolution $\Delta \text{CR}_{\text{knm}}$ for operational task type k, scenario n, and measurement m, which is used to calculate the classification performance for weather surveillance, is estimated as

$$\Delta R = c_w / (2B_k) \tag{15}$$

$$\Delta CR_{\text{knm}} = 2R_{\text{knm}} \tan 0.5\theta_r \tag{16}$$

where B_k is the used bandwidth for operational task k. The radar accuracy in spherical coordinates, which are eventually transformed to estimate the measurement accuracy in perspective of the effector, is given by [42]

$$\sigma_{Rs}(k, n, m) = \frac{c_w}{2B_k \sqrt{2(\text{ISNR})_{\text{knm}}}} \tag{17}$$

$$\sigma_{As}(k, n, m) = \frac{\theta_r}{S_{\text{mono}} \sqrt{2(\text{ISNR})_{\text{knm}}}} \tag{18}$$

where σ_{Rs} is sensor accuracy in range, σ_{As} is sensor accuracy in azimuth, B_k is the used bandwidth for search in the framework of operational task k, $(\text{ISNR})_{\text{knm}}$ integrated-signal-to-noise ratio [42] at measurement m for operational task k, and S_{mono} is the monopulse pattern difference slope.

B. Radio Communication

A radio communication link, as shown in Fig. 3, is concurrently required for operational tasks $k = 3, 4$ (i.e., crowd control and drone control). The links are modeled by assuming a stationary free space radio channel [43], [44]

$$P_R(k) = P_T(k) G_T(k) G_R(k) \left(\frac{\lambda_k}{4\pi d_{\text{link}}} \right)^2 \tag{19}$$

where $P_R(k)$ is the received power, $P_T(k)$ is the transmitted power, $G_T(k)$ is the antenna gain for transmission, $G_R(k)$ is the receive antenna gain, λ_k is the communication wavelength, and d_{link} is the range to the drone as shown in Fig. 3.

The signal-to-noise ratio at the receiver input is given by

$$\text{SNR}_R(k) = \frac{P_R(k)}{NL}. \tag{20}$$

Based on the SNR_R it is possible to compute the theoretical bit error rate (BER) [43]. If a binary shift keying modulation scheme is assumed, BER is estimated as

$$\text{BER}(k) = Q\left(\sqrt{\frac{2E_b}{N_0}} \right) = Q\left(\sqrt{\frac{2\text{SNR}_R(k)}{R_b(k)}} \right) \tag{21}$$

where Q is an error function of [43], E_b the energy per bit, and N_0 the power spectral density of the additive white Gaussian noise assumed in the underlying model [43].

The binary BCH codes [45] is used as forward error correction scheme to be more resilience against bit errors. As a results, the packet error rate (PER) is given by

$$\text{PER}(k) = 1 - \sum_{j=0}^{t(k)} \binom{n(k)}{j} \text{BER}(k)^j (1 - \text{BER}(k))^{n(k)-j} \tag{22}$$

where $t(k)$ is the maximum number of error bits and $n(k)$ is the total size of the packet including the overhead. The block length $n(k)$, which should be larger than the original packet size, is given by

$$n(k) = 2^{m(k)} - 1 \tag{23}$$

where m is a positive integer larger than 3. A detailed table is given in [45] of possible binary BCH codes, but in order to be concise the maximum number of error bits is estimated as

$$t(k) = \left\lfloor \frac{n(k) - p(k)}{m(k)} \right\rfloor \tag{24}$$

where $p(k)$ is the number of data bits of the original packet. Operator $\lfloor . \rfloor$ is a floor function. If the correction scheme is not used for task $k = 3, 4$, then $n(k) = p(k)$ and $t(k) = 0$.

The total number of bits including all overhead is given by

$$N_b(k) = N_{\text{im}}(k) \frac{n(k)}{p(k)} \tag{25}$$

where $N_{\text{im}}(k)$ is the size in bits of the original message. The probability that this complete message is successfully

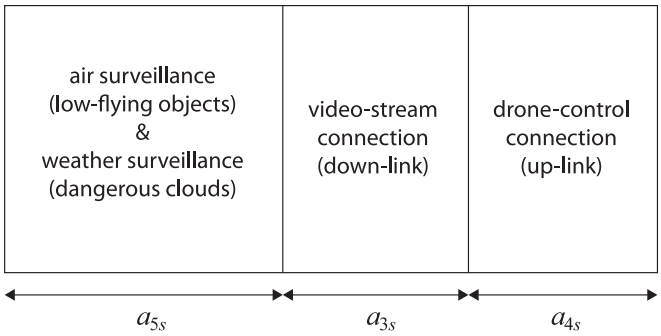

Fig. 4. Allocation of RF antenna elements.

transmitted and received is given by

$$\text{MSR}(k) = (1 - \text{PER}(k))^{N_{\text{im}}(k,x)/p(k)}. \tag{26}$$

C. Reconfigurable RF Front End

Each RF front end $s = 1, 2, 3, 4$ is physically divided in three parts as illustrated in Fig. 4. The communication up and down links receive their own part. The air and weather surveillance have to share their time budget. Parameters a_{1s} and a_{2s} control the division of time budget over tasks $k = 1, 2$. Parameters a_{3s}, a_{4s}, and a_{5s} control the division of antenna elements over the tasks. Because the resources are limited, the allocations are interdependent: $a_{1s} + a_{2s} = 1 = a_{3s} + a_{4s} + a_{5s}$.

The selected allocation influences the characteristics of surveillance and communication for each RF front end s

$$P_{S-s} = a_{5s} P_0 \tag{27}$$

$$G_{S-s} = a_{5s} G_0 \tag{28}$$

$$\theta_s = \min\left(\left[\frac{\theta_0}{a_{5s}}, 90\right]\right) \tag{29}$$

$$P_{T-s}(k) = \begin{cases} P_{T-\text{drone}}, & \text{if } k = 3 \text{ (down link)} \\ a_{4s} P_0, & \text{if } k = 4 \text{ (up link)} \end{cases} \tag{30}$$

$$G_{T-s}(k) = \begin{cases} G_{T-\text{drone}}, & \text{if } k = 3 \text{ (down link)} \\ a_{4s} G_0, & \text{if } k = 4 \text{ (up link)} \end{cases} \tag{31}$$

$$G_{R-s}(k) = \begin{cases} a_{3s} G_0, & \text{if } k = 3 \text{ (down link)} \\ G_{R-\text{drone}}, & \text{if } k = 4 \text{ (up link)} \end{cases} \tag{32}$$

where P_0 is the total available power at the RF front end, G_0 the antenna gain of the complete array, θ_0 is the antenna beamwidth of the complete array, and $P_{T-\text{drone}}$, $G_{T-\text{drone}}$, and $G_{R-\text{drone}}$ are the drone's transmit power, transmit antenna gain, and receive antenna gain, respectively.

VI. Resource Management Demonstration

The operational task performance QoS_{zk} is linked to the expected mission success U_E in Section II and the system parameters are linked to QoS_{zk} in Section V and the Appendices. As a result, expected mission success can be maximized by adapting the system parameters, as demonstrated in the following.

A. Operational Story

The operational tasks $k = 1, 2, 3$ (i.e., air defense, storm protection, and crowd control) are generated for the assets $z = 1, 2, 3$ (i.e., main tent, communication base station, and VIP). Operational task $k = 4$ (i.e., drone flight) is only generated for asset $z = 4$ (i.e., camera-equipped drone). Many test scenarios are defined, and the likelihood of scenarios $P(X_{kn}|E_k)$ is assumed uniform. When the mission starts, the threat assessment is defined as $P(E_1) = 0.3$, $P(E_2) = 0$, $P(E_3) = 0.5$, and $P(E_4) = 0$. Furthermore, the organization has uniformly prioritized the assets: $u_z = 1$ for all z.

Many aspects (e.g., positions of the VIP and drone) will change during the mission. The following changes in the expectations are added, where t_0 is the moment that the mission starts and T_M is the total mission time.

1) New intelligence is received at $t_1 = t_0 + 0.2T_M$ via twitter that an ultralight air object is observed near the event. Because of this, $P(E_1)$ increases to 0.9.
2) The drone fails to cope with a situation at $t_2 = t_0 + 0.3T_M$ and the drone operator should intervene. Because of this, $P(E_4)$ becomes 1 until the drone is secured.
3) An ultralight air object becomes detectable at $t_3 = t_0 + 0.5T_M$. After detection, $P(E_1)$ increases to 1. After the interception, $P(E_1)$ is decreased to 0.9 again.
4) The weather-agency reports an increased probability of a storm coming from the West near the event at $t_4 = t_0 + 0.8T_M$. Because of this, $P(E_2)$ increases to 0.8.

When an ultralight object is detected after moment t_3, a mission critical question has to be answered. Namely, can we expect more ultralight objects, and if so, can we neutralize them with the remaining effectors? If no more ultralight objects are expected or no effector resources are available to intercept another one, then spending resources on finding new ultralights is useless. In that case, the full air surveillance capacity should be allocated to track the detected target.

It is assumed in this simulation that a detected object results in three extra potential trajectories for QoS_{zk} evaluation. Namely, from the current object's location toward the three assets $z = 1, 2,$ and 3. The probability $P(X_{kn}|E_k)$ that an attacking object takes this path kn for each of these three paths is assumed to be equal to 0.25. Thus, there is a probability of $1 - (3 * 0.25) = 0.25$ that the detected object is actually not successfully attacking, and that another object attacks.

As a result, the system will mainly focus on a detected object, but not exclude the possibility that an undetected object attacks. Of course, the complexity of the case study can be increased by adding extra effectors, but the proposed principle to tradeoff between searching new objects and intercepting targets remains the same: Maximize U_E.

B. Algorithm Strategy

The MATLAB Global Optimization Toolbox is exploited to maximize U_E and U_Q. We used a two-step process. First a multistart gradient-search algorithm is applied to obtain an optimized allocation solution. This output is used as input for a pattern-search algorithm as a starting point.

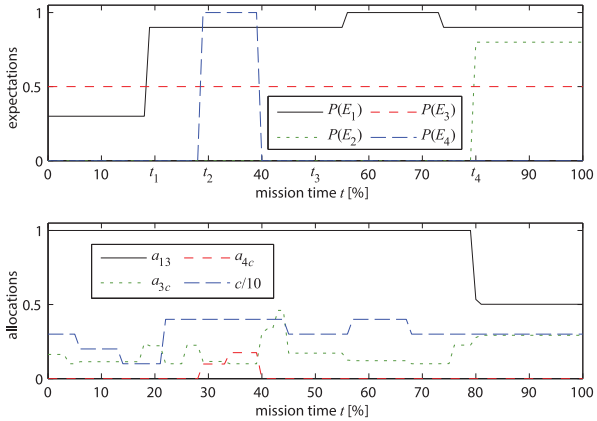

Fig. 5. Expectations and allocation of resources.

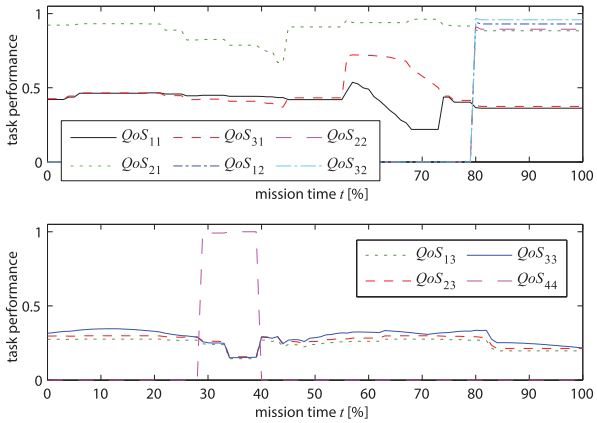

Fig. 6. Provided performances for operational tasks.

A number of system parameters is assumed reconfigurable to demonstrate the mission-driven optimization. Allocation a_{1s} is optimized for each sensor s. Allocations a_{3s} and a_{4s} are equal to zero and not optimized, except when $s = c$, where index c relates to RF front-end index s that covers the drone position and can be selected to communicate with this moving platform. The surveillance part is optimized for each sensor s: volume range $R_{\text{un}}(k, s)$ and number of pulses n_{ks} for operational tasks $k = 1$ and 2. The communication part is optimized using the following parameters: average number of bits per pixel B_{im}, communication bit-rate $R_b(k)$, and error bit control $m(k)$ and $p(k)$ for operational tasks $k = 3$ and 4.

C. Management Evaluation

The threat assessment and automatic management as function of mission time is depicted in Fig. 5. The first subplot shows the expectations $P(E_k)$. The second subplot shows a few system parameters. Only a_{1s} for front end $s = 3$, which is pointing to the West, is plotted, because the expected storm is coming from the West. The system is continually reconfigured based on expectations $P(E_k)$ and the dynamic situation. This can also be seen in Fig. 6. The tasks performances QoS_{zk} values are constantly adapted during the mission, depending on the situation and expectations.

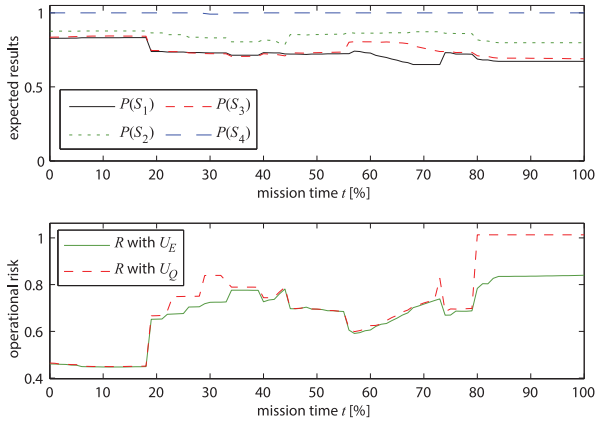

Fig. 7. Expected mission results and operational risk.

Fig. 7 displays the expected results for each asset z and risk (linearly related to expected utility [34]) during the mission. The first three assets $z = 1, 2, 3$ are roughly equally protected, which is mainly due to the fact that they are equally vulnerable and have the same threats to deal with. Asset $z = 4$ is completely different, because the drone is only facing the threat of incorrect flight control.

The difference between a heuristic and the proposed model-based solution can be explained by considering moment t_4. A heuristic solution could enable the weather surveillance using some simple rule, such as for $s = 3$: if $P(E_2) > 0$, then $a_{2s} = 0.3$, else $a_{2s} = 0$. However, then the actual argument for enabling weather surveillance remains unstated. Instead, the proposed solution is based on models. In the employed models, it is described that as soon as weather surveillance sensing capability is enabled, the detection of coming severe storm initiates an evacuation action, and therefore, the damage to the assets that are vital to the mission can be reduced. Thus, the mission-driven concept enables weather surveillance at moment t_4, not because of any expert's opinion, but to maximize mission success expectations U_E.

The operational risk R after traditional task-driven optimization is also displayed in Fig. 7. The mission-driven solution results in the lowest risk values, and provides expected-utility U_E values that are on average 6% higher, with a maximum up to 23%, than the task-driven method. Note, the QoS_{zk} used in this task-driven method already expresses operational relevance, and is not describing sensing or system characteristics. Moreover, this QoS_{zk} is comparable between heterogeneous tasks, which allows meaningful summation. Therefore, the used task-driven objective function is already much better in comparison to many that can be found in the literature. Moreover, as shown in Section III, the improvement of using the mission-driven solution can be infinitely high.

VII. Conclusion

The developed mission-driven resource management solution directly defines the end-user's mission as the optimization objective for reconfigurable sensing systems. As a result, the process is not driven by technical characteristics, lookup tables,

rules-of-thumb, task priorities, and/or artificial quality measures, but by mission success. Any decision (e.g., tradeoffs between many types of tasks, graceful performance and degradation) can be made based on a single objective function, making the optimization clear and transparent. Thus, the system effectiveness is not measured by an abstract information measure or technical estimation error, but by how much a sensing system is expected to contribute to the mission. The obtained performance with a mission-driven approach in comparison to a task-driven one cannot be worse, is at least equal, and potentially much better.

The presented framework allows to define various threats, heterogeneous tasks, (reconfigurable) sensing resources, and mission success in a consistent manner. New aspects can be easily added. The result of permanent maximization of mission success expectations is that the systems are automatically, quickly and accurately adapted to fast changing missions, environments, and threats. As a result, the end user is supported to execute the mission, such as the security of a large event, in the most effective way.

Appendix A
Probability of Successful Air Defense

This appendix estimates the probability $P(S_{z1}|X_{1n})$ that asset z is secured against threatening air objects in scenario n of operational task $k = 1$. To be concise, only scenarios with a single object that is targeting a single asset are considered. An air object is able to take off from outside the event area, and then, fly toward an asset as example trajectories show in Fig. 2. The boundary drawn around each asset indicates the positions of an air object at which the effector can still initiate an in-time interception.

Successful interception of threatening objects requires that supporting information is provided by the sensors to the effector that has the capability to intercept air units. Let us assume that the sensor can detect and track air units, and the effector uses the sensed information (e.g., object position) to intercept the dangerous object (e.g., the object is unexpected and/or does not respond to interrogation).

When the sensor is performing air surveillance, the effector is standing-by, and an air object is flying some trajectory n, then there are many possible outcomes. Assume that the sensor executes track-while-scan surveillance and M_n is equal to the total number of possible object scans during scenario n. For every scan number $m = 1 \dots M_n$, there is a probability P_{knm} that the object is detected. It is assumed that an initial detection is promoted to a confirmed track when the object is detected twice in sequence. Further, the sensor cues a target to the effector for interception at the moment of a confirmed track if there is no indication that the object is friendly.

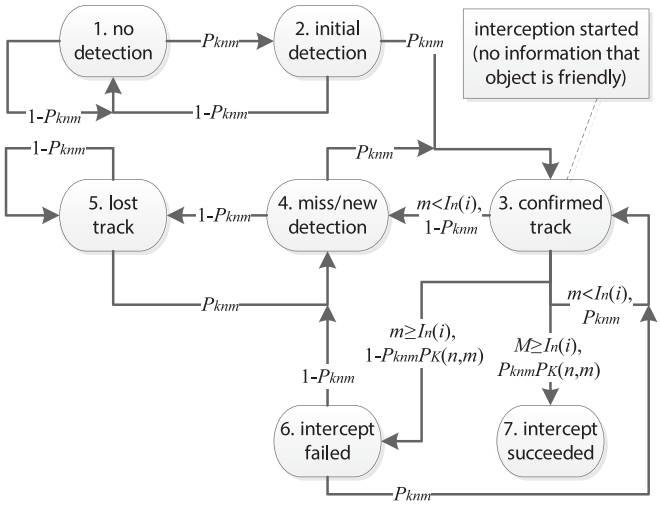

Fig. 8. Markov chain of detection, tracking, and interception process.

Given the described system concept, Fig. 8 shows a Markov chain [46] for calculating possible outcomes for a given scenario. The states of the Markov chain should be understood from the threatening object perspective (e.g., they do not express the sensor states). The chain is synchronized with the sensor scans $m = 1 \dots M_n$. When an object starts an attack, the attacking process starts in state "1. no detection." At each step m, the state can change, which depends on the depicted probabilities. If $m > M_n$, then the process stops, because this means that the system did not intercept the threat in time. Only if the process ends up in the "7. intercept succeeded" state, the system successfully coped with the scenario.

The probability that the process ends in state $d = 7$ is calculated for each scenario n. Recursive formula (33), shown at the bottom of the page, is used for this purpose where L_n is the latest possible moment for the sensor to cue the object to an effector for timely interception, $I_n(i)$ is the first moment that the object is in the interception range of the effector, i is the moment that the effector started to move toward the object, $P_K(m, n)$ is the probability that the effector intercepts an object when it attempts to intercept at moment m, and d indicates the states

$$P_I(m,i,d) = \begin{cases} 0, & \text{if } m > M_n \\ 0, & \text{elseif } m > L_n \text{ and } d = 1,2 \\ P_{\text{knm}} P_I(m+1,m,2) + (1-P_{\text{knm}}) P_I(m+1,m,1), & \text{elseif } d = 1 \\ P_{\text{knm}} P_I(m+1,m,3) + (1-P_{\text{knm}}) P_I(m+1,m,1), & \text{elseif } d = 2 \\ P_{\text{knm}} P_I(m+1,i,3) + (1-P_{\text{knm}}) P_I(m+1,i,4), & \text{elseif } m < I_n(i) \text{ and } d = 3 \\ P_{\text{knm}} P_K(m,n) + (1-P_{\text{knm}} P_K(m,n)) P_I(m+1,i,6), & \text{elseif } m \geq I_n(i) \text{ and } d = 3 \\ P_{\text{knm}} P_I(m+1,i,3) + (1-P_{\text{knm}}) P_I(m+1,i,5), & \text{elseif } d = 4 \\ P_{\text{knm}} P_I(m+1,i,4) + (1-P_{\text{knm}}) P_I(m+1,i,5), & \text{elseif } d = 5 \\ P_{\text{knm}} P_I(m+1,i,3) + (1-P_{\text{knm}}) P_I(m+1,i,4), & \text{otherwise (if } d = 6) \end{cases} \quad (33)$$

and corresponds to the numbers in Fig. 8. To clarify, $P_I(m,i,d)$ is the probability that the object will be intercepted in the future before M_n+1 given the current situation described by m, i, and d.

Note, because (33) is recursive, dynamic programming [47] can be used to calculate $P_I(m,i,d)$. In this way, intermediate outputs of $P_I(m,i,d)$ are saved and reused, required time is traded against required memory and the computation of $P_I(m,i,d)$ is significantly accelerated.

The following formulas are used to estimate the task performance for scenario n related to asset z

$$P(S_{z1}|X_{1n}) = P_I(1,1,1) \tag{34}$$

$$I_n(i) = N_{\text{RT}}(i) + i \tag{35}$$

where N_{RT} is the remaining number of sensor revisits after a confirmed detection at moment i. Valuable N_{RT} depends on the remaining time $t_n(i)$ after starting an interception at moment i, which is estimated by solving these equations based on geometry

$$\begin{aligned} v_n\sin(\alpha_n)t_n(i) + x_n(i) &= (v_e t_n(i) + R_e)\sin(\epsilon_n(i)) + x_b \\ v_n\cos(\alpha_n)t_n(i) + y_n(i) &= (v_e t_n(i) + R_e)\cos(\epsilon_n(i)) + y_b \end{aligned} \tag{36}$$

where v_n is the velocity of the threatening object, α_n is its attacking angle, $x_n(i)$ and $y_n(i)$ represent the object's position at moment i, v_e is the effector's velocity, R_e is the effector's interception range, $\epsilon_n(i)$ is the interception angle if the object is cued to the effector at i, and x_b and y_b the location of the effector's base. The aforementioned equation is assumed to be also appropriate to determine the effector's and object's positions for extra interception attempts after an initially failed one.

The probability that a tracked object is intercepted depends on the data (e.g., estimation error) provided by the sensor:

$$\begin{aligned} P_K(n,m) &= \prod_{j=1}^{2} \int_{-\frac{\vartheta_j(n,m)}{2}}^{\frac{\vartheta_j(n,m)}{2}} f(v,\sigma_j(n,m),0)\mathrm{d}v \\ &= \prod_{j=1}^{2} \text{erf}\left(\frac{\vartheta_j(n,m)}{2^{3/2}\sigma_j(n,m)}\right) \end{aligned} \tag{37}$$

where $\vartheta_j(n,m)$ is the object size, $\sigma_j(n,m)$ is the observation's standard deviation in the effector's intercept angle Polar coordinate j during measurement m of scenario n, $f(v,\sigma,\mu)$ is the normal probability density of variable v with standard deviation σ and mean μ, and erf(.) is the error function.

Accuracy $\sigma_j(n,m)$ is measured in perspective of the effector. However, the measurements are executed by a sensor that has another position than the effector. Thus, accuracies σ_{Rs} and σ_{As} related to the sensor measurements, as explained in Appendix V, have to be transformed. The unscented transform [48], which translates a set of sigma points to the new domain, can be used for this purpose.

Appendix B
Probability of Successful Weather Alarm

This appendix estimates probability $P(S_{z2}|X_{2n})$ that asset z is protected against a severe storm scenario n (e.g., heavy precipitation and wind gusts). The scenario is based on the analysis of past weather calamities and safety services have confirmed that a sudden storm may disturb the event and harm the assets. Fig. 2 shows the impact area for an example storm scenario.

External weather reports (e.g., national weather service) provide rough forecasts (couple of hours in advance) about upcoming storms. However, this forecast is not precise enough to estimate the necessity of an action (e.g., event evacuation). Therefore, if a potentially harmful storm is predicted, an accurate on-site radar observation system is needed for now-casting [49]. Now-casting estimates in more detail (locations, intensity, etc.) the weather and allows prediction over up to 10 min to support emergency decisions [49].

If an atmospheric object is classified as dangerous by the on-site sensor, an early warning is transmitted to the assets. Note, a warning is activated only once. The assets can then be evacuated or prepared for impact. Each storm scenario n describes 1) the area of impact, and thus, which asset(s) z can be damaged without evacuation, 2) the reflectivity (i.e., detectability) of the storm as function of time, and 3) the remaining time before the storm impacts after the initial warning issued by the external weather forecast. The probability that a timely warning is given to asset z is calculated as follows:

$$P(S_{z2}|X_{2n}) = \sum_{m=1}^{M_{2n}} P_W(n,m)P_P(z,m) \tag{38}$$

where M_{2n} is the number of sensor measurements before the storm impacts the event for scenario n, $P_W(n,m)$ is the probability that a warning is issued during weather surveillance measurement m during scenario n, and $P_P(z,m)$ is the probability that asset z could be prepared for impact given a warning at moment m. Note that M_{2n} depends on the sensor revisit time for weather surveillance.

The better the weather surveillance, the higher the quality of now-casting, the more time an asset statistically has to prepare before impact. The probability that an alarm is broadcasted to the assets is estimated as

$$\begin{aligned} &P_W(n,m) \\ &= \begin{cases} P_C(n,m), & \text{if } m=1 \\ P_C(n,m)\left(1-\sum_{m_0=1}^{m-1} P_W(n,m_0)\right), & \text{else} \end{cases} \end{aligned} \tag{39}$$

where $P_C(n,m)$ is the probability that the dangerous atmospheric object is classified as dangerous at measurement m during scenario n. The following function is employed to estimate the classification performance:

$$\begin{aligned} P_C(n,m) = P_{\text{knm}}&\left(1 - S(\Delta R - \Delta F)\right) \\ &\times \left(1 - S(\Delta CR_{\text{knm}} - \Delta F)\right) \end{aligned} \tag{40}$$

where P_{knm} is the probability that the cloud is detected, ΔR is the range resolution, ΔF is a reference range resolution for proper classification, and ΔCR_{knm} is the cross-range resolution for cloud in scenario n at measurement m. The sigmoid function

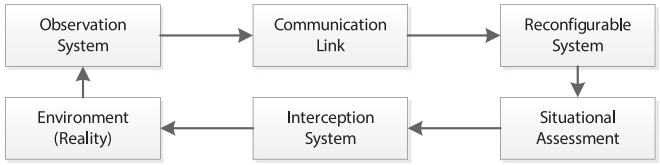

Fig. 9. Overview of crowd surveillance and control.

S is defined as follows:

$$S(t) = \frac{1}{1 + \exp(-\delta t)} \tag{41}$$

where δ is a parameter to modify the shape of the curve.

More preparation time means a higher probability that an asset survives an impact. Function $S(A, B)$ is reused to model the probability that an asset is able to prepare for impact

$$P_P(z, m) = S((M_{2n} - m)\,\mathrm{RT}_2 - \mathrm{PT}_z) \tag{42}$$

where RT_2 is the revisit time of the weather surveillance and PT_z is the required time for asset z to prepare for impact in order to have a chance of 50% that it is undamaged. Note, parameter PT_z is not a fixed requirement, but it shapes $P_P(z, m)$.

Appendix C
Probability of Successful Crowd Control

Probability $P(S_{z3}|X_{3n})$ that asset z is protected during scenario n of operational task $k = 3$ is calculated in this appendix. Crowds of people may pose a threat to the assets by agitated behavior and creating chaos. A camera-equipped drone is flying over the event area to identify abnormal behavior of crowds (e.g., with image pattern recognition methods) and inappropriate activities should be stopped by the effectors (e.g., police officers). Fig. 2 shows a boundary around each asset that indicates the positions of a threatening crowd at which the surface effector can still initiate an timely reaction.

The assumed crowd-control architecture is depicted in Fig. 9. The camera-equipped drone (i.e., observation system) is fully allocated to scan the crowd on the ground (i.e., environment) and supporting surface surveillance. The sensed data are transferred (i.e., communication link) to the base station (i.e., reconfigurable system) that directly communicates it to the security officers on the ground. These officers analyze (i.e., situational assessment) and use the data to identify and intercept threatening crowds (i.e., interception system). As a result, they change the situation (i.e., environment).

The shortest path from the crowd to the assets is a straight line, so the shortest reaction time comes from this path. If the crowd is not moving in a straight line, more time will be available. The probability that the group is detected in time is estimated as follows:

$$P(S_{z3}|X_{3n}) = P(S_4)\int_{r_l(z,n)}^{\infty} P_{\mathrm{un}}(z, n, r)\mathrm{CDP}\left(\frac{r - r_l(z, n)}{v_{\mathrm{crowd}}}\right)\mathrm{d}r \tag{43}$$

where $P(S_4)$ is the probability that the drone is in operation, $P_{\mathrm{un}}(z, n, r)$ is the probability that the crowd unmasks (i.e., is identifiable as threatening) as a function of distance r to the asset z of scenario x, $\mathrm{CDP}(T)$ is the cumulative detection probability, which is the probability of one or more detections during time window $T = (r - r_l(z, n))/(v_{\mathrm{crowd}})$, that the crowd is agitated, $r_l(z, n)$ is the distance between asset z and the crowd of scenario n at which the effector has the last possibility to start a timely interception, and $v_{\mathrm{crowd}}(n)$ is the expected velocity of the crowd of scenario n.

A normal distribution is used for estimating the unmask probability as function of distance to asset z in scenario n

$$P_{\mathrm{un}}(z, n, r) = \frac{1}{\sigma_{zn}\sqrt{2\pi}}\exp\left(-\frac{(r - \mu_{zn})^2}{2\sigma_{zn}^2}\right) \tag{44}$$

where μ_{zn} is the mean distance and σ_{zn} is the standard deviation for asset z and scenario n where a threatening crowd can unmask.

Probability $\mathrm{CDP}(T)$ is modeled [50] as follows:

$$\mathrm{CDP}(T) = 1 - \exp\left(-P_{\mathrm{do}}P_{\mathrm{id}}\frac{v_{\mathrm{drone}}w_c}{A_e}T\right) \tag{45}$$

where P_{do} is the probability that a captured image of the sensor is successfully downloaded to the police officers, P_{id} is the identification (by the police officers) probability when the crowd has become detectable and within the camera's field of view, v_{drone} is the drone search speed, w_c is the camera sweep width, A_e the area of the event, that is searched by the sensor-equipped drone, and T the search time. The sensor sweep width is estimated as follows:

$$w_s = 2R_{\mathrm{id}}\tan(0.5\alpha_s) \tag{46}$$

where α_s is the camera field of view angle and R_{id} is the sensor-surface range.

Probability P_{id} is dependent on the image quality that the sensor operator is analyzing. The following metric is used based on experimental studies [51]:

$$P_{\mathrm{id}} = \frac{\left(\frac{N_{\mathrm{resolved}} - 2.6}{20.8}\right)^E}{1 + \frac{N_{\mathrm{resolved}} - 2.6}{20.8}^E} \tag{47}$$

$$E = 1.33 + 0.23\frac{N_{\mathrm{resolved}} - 2.6}{20.8} \tag{48}$$

where N_{resolved} is the number of resolved cycles on target. Parameter N_{resolved} is given as [51]

$$N_{\mathrm{resolved}} = \frac{\sqrt{A_{\mathrm{id}}}}{R_{\mathrm{id}}}\int_{C_{\mathrm{TGT}} > \mathrm{CTF}_{\mathrm{sys}}(\epsilon)}\left(\frac{C_{\mathrm{TGT}}}{\mathrm{CTF}_{\mathrm{sys}}(\epsilon)}\right)^{0.5}\mathrm{d}\epsilon \tag{49}$$

where A_{id} is the crowd-size, $CTF_{\mathrm{sys}}(\epsilon)$ is the eye's contrast threshold function (values can be found in [51]), and C_{TGT} is the target to background contrast.

As discussed, the image is captured by the sensor and transmitted over the communication channel. The properties of this communication channel are adaptable, and therefore, the transmitted image quality is adaptable. In this paper, C_{TGT} depends

on the quality of the transmitted image

$$C_{\text{TGT}} = \left(\frac{L_{\text{im}}}{L_{\text{un}}}\right)^{\epsilon_L} \left(\frac{B_{\text{im}}}{B_{\text{un}}}\right)^{\epsilon_B} C_{\text{TGT-0}}\beta^{R_{\text{id}}} \tag{50}$$

where $C_{\text{TGT-0}}$ is the zero range contrast, β is the transmission loss, L_{im} and L_{un} is the number of horizontal or vertical lines (we assume a 1:1 ratio image) in the compressed and uncompressed image, respectively, B_{im} and B_{un} the average number of bits for a pixel in the compressed and uncompressed image, respectively, and ϵ_L and ϵ_B are scalars indicating the picture degradation due to image compression.

The probability that at least one relevant image of an area within the sensor field of view is successfully transmitted to the reconfigurable system is estimated as

$$P_{\text{do}} = 1 - (1 - \text{MSR}(k))^{f_{\text{frame}} \frac{w\ s}{v\ \text{drone}}} \tag{51}$$

where $\text{MSR}(k)$ is the message success rate (probability to successfully download a single image) for operational task $k = 3$, and f_{frame} is the number of transmitted frames per second. The number of frames is given by

$$f_{\text{frame}} = \frac{R_b(k)}{N_b(k)} \tag{52}$$

where $R_b(k)$ is the selected communication bit rate for operational task k and $N_b(k)$ the number of bits per image/packet including the overhead. The number of transmitted bits for a single image without the overhead is given by

$$N_{\text{im}}(k) = L_{\text{im}}^2 B_{\text{im}}. \tag{53}$$

APPENDIX D
PROBABILITY OF SUCCESSFUL DRONE FLIGHT

This appendix calculates probability $P(S_{z4}|X_{4n})$ that the drone is successfully controlled during dangerous air scenario n. The automatic pilot may fail to act correctly in unusual air situations. In such situations, the drone operator should be able to manage the drone remotely by sending control messages to the drone and avoid a potential accident.

The performance evaluation for this last operational task is concisely discussed. The probability that the drone remains on the predetermined path given a situation that the operator intervenes is calculated as follows:

$$P(S_{z4}|X_{4n}) = \exp\left(-\text{MSR}(k,n)\frac{R_b(k)}{N_b(k,n)}AT_n\right) \tag{54}$$

where $\text{MSR}(k,n)$ is the probability that a message is successfully received for operational task $k = 4$, $N_b(k,n)$ is the size of the message in bits including all overhead, and AT_n is the time available during scenario n to transmit the instructions before an accident.

ACKNOWLEDGMENT

The authors would like to thank Prof. P. van Genderen (Delft University of Technology), Dr. H. Driessen (Thales Nederland), and N. Sawaryn (Thales Nederland) for providing feedback to enhance this research; M. Wiebes and T. Holtslag (Dutch National Police) for discussing operational issues related to large events; S. Drude (NXP Semiconductors) for supporting the modeling of the communication channel; and J. H. Weber (Delft University of Technology) for discussing the error correcting codes. They also want to thank their colleagues F. Katsilieris and A. Narykov for providing feedback on this paper.

REFERENCES

[1] R. Popoli and S. Blackman, "Expert system allocation for the electronically scanned antenna radar," in *Proc. Amer. Control Conf.*, 1987, pp. 1821–1826. [Online]. Available: http://ieeexplore.ieee.org/xpl/articleDetails.jsp?arnumber=4789608

[2] J. M. Molina, J. G. Herrero, F. J. Jimenez, and J. R. Casar, "Fuzzy reasoning in a multiagent system of surveillance sensors to manage cooperatively the sensor-to-task assignment problem," *Appl. Artif. Intell.*, vol. 18, no. 8, pp. 673–711, 2004.

[3] S. Miranda, C. Baker, K. Woodbridge, and H. Griffiths, "Knowledge-based resource management for multifunction radar: A look at scheduling and task prioritization," *IEEE Signal Process. Mag.*, vol. 23, no. 1, pp. 66–76, Jan. 2006.

[4] M. de Vilmorin, E. Duflos, and P. Vanheeghe, "Radar optimal times detection allocation in multitarget environment," *IEEE Syst. J.*, vol. 3, no. 2, pp. 210–220, Jun. 2009.

[5] A. Charlish, "Autonomous agents for multi-function radar resource management," Ph.D. dissertation, Dept. Electron. Elect. Eng., Univ. College London, London, U.K., 2011.

[6] C. Baker and A. Hume, "Netted radar sensing," *IEEE Aerosp. Electron. Syst. Mag.*, vol. 18, no. 2, pp. 3–6, Feb. 2003.

[7] J. Wintenby and V. Krishnamurthy, "Hierarchical resource management in adaptive airborne surveillance radars," *IEEE Trans. Aerosp. Electron. Syst.*, vol. 42, no. 2, pp. 401–420, Apr. 2006.

[8] C. Yang, L. Kaplan, and E. Blasch, "Performance measures of covariance and information matrices in resource management for target state estimation," *IEEE Trans. Aerosp. Electron. Syst.*, vol. 48, no. 3, pp. 2594–2613, Jul. 2012.

[9] J. L. Williams, "Information theoretic sensor management," Ph.D. dissertation, Dept. Elect. Eng. Comput. Sci., Massachusetts Inst. Technol., Cambridge, MA, USA, 2007.

[10] Y. Zhang and Q. Ji, "Efficient sensor selection for active information fusion," *IEEE Trans. Syst., Man, Cybern. B, Cybern.*, vol. 40, no. 3, pp. 719–728, Jun. 2010.

[11] M. Kolba, W. Scott, and L. Collins, "A framework for information-based sensor management for the detection of static targets," *IEEE Trans. Syst., Man Cybern. A, Syst., Humans*, vol. 41, no. 1, pp. 105–120, Jan. 2011.

[12] E. Jaska, "Optimal power-aperture balance," in *Proc. IEEE Radar Conf.*, 2003, pp. 203–209.

[13] B. Dieber, C. Micheloni, and B. Rinner, "Resource-aware coverage and task assignment in visual sensor networks," *IEEE Trans. Circuits Syst. Video Technol.*, vol. 21, no. 10, pp. 1424–1437, Oct. 2011.

[14] M. Perillo and W. Heinzelman, "Optimal sensor management under energy and reliability constraints," in *Proc. IEEE Wireless Commun. Netw.*, vol. 3, 2003, pp. 1621–1626.

[15] J. Glass, W. Blair, and Y. Bar-Shalom, "Optimizing radar signal to noise ratio for tracking maneuvering targets," in *Proc. Int. Conf. Inf. Fusion*, 2014, pp. 1–7. [Online]. Available: http://ieeexplore.ieee.org/xpl/articleDetails.jsp?arnumber=6916206

[16] J. Hansen, R. Rajkumar, J. Lehoczky, and S. Ghosh, "Resource management for radar tracking," in *Proc. IEEE Conf. Radar*, 2006, pp. 140–147.

[17] M. Zink, E. Lyons, D. Westbrook, and J. Kurose, "Closed-loop architecture for distributed collaborative adaptive sensing of the atmosphere: Meteorological command and control," *Int. J. Sensor Netw.*, vol. 7, no. 1, pp. 4–18, 2010.

[18] A. Irci, A. Saranli, and B. Baykal, "Study on Q-RAM and feasible directions based methods for resource management in phased array radar systems," *IEEE Trans. Aerosp. Electron. Syst.*, vol. 46, no. 4, pp. 1848–1864, Oct. 2010.

[19] C.-G. Lee, "A novel framework for quality-aware resource management in phased array radar systems," in *Proc. IEEE Real Time Embedded Technol. Appl. Symp.*, 2005, pp. 322–331.

[20] T.-H. Lan and A. Tewfik, "A resource management strategy in wireless multimedia communications-total power saving in mobile terminals with a guaranteed QoS," *IEEE Trans. Multimedia*, vol. 5, no. 2, pp. 267–281, Jun. 2003.

[21] A. Mehra, A. Indiresan, and K. Shin, "Structuring communication software for quality-of-service guarantees," *IEEE Trans. Softw. Eng.*, vol. 23, no. 10, pp. 616–634, Oct. 1997.
[22] J. Yoon, W.-Y. Shin, and H. S. Lee, "Energy-efficient opportunistic interference alignment," *IEEE Commun. Lett.*, vol. 18, no. 1, pp. 30–33, Jan. 2014.
[23] J. Cai, X. Shen, and J. W. Mark, "Downlink resource management for packet transmission in OFDM wireless communication systems," *IEEE Trans. Wireless Commun.*, vol. 4, no. 4, pp. 1688–1703, Jul. 2005.
[24] A. Moller and U. Jonsson, "Input-output analysis of power control in wireless networks," *IEEE Trans. Autom. Control*, vol. 58, no. 4, pp. 834–846, Apr. 2013.
[25] S. Abedi, "Efficient radio resource management for wireless multimedia communications: A multidimensional QoS-based packet scheduler," *IEEE Trans. Wireless Commun.*, vol. 4, no. 6, pp. 2811–2822, Nov. 2005.
[26] S. Ghosh, R. Rajkumar, J. Hansen, and J. Lehoczky, "Scalable resource allocation for multi-processor QoS optimization," in *Proc. 23rd Int. Conf. Distrib. Comput. Syst.*, 2003, pp. 174–183.
[27] J. Hansen and S. Hissam, "Assessing QoS trade-offs for real-time video," in *Proc. IEEE Int. Symp. Workshops World Wireless, Mobile Multimedia Netw.*, 2013, pp. 1–6.
[28] S. L. C. Miranda, C. Baker, K. Woodbridge, and H. Griffiths, "Fuzzy logic approach for prioritisation of radar tasks and sectors of surveillance in multifunction radar," *IET Radar, Sonar Navigat.*, vol. 1, no. 2, pp. 131–141, Apr. 2007.
[29] F. Bolderheij, "Mission-driven sensor management—Analysis, design, implementation and simulation," Ph.D. dissertation, Int. Res. Centre Telecommun. Radar, Delft Univ. Technol., Delft, Netherlands, 2007.
[30] H. Kloeden, N. Damak, R. Rasshofer, and E. Biebl, "Sensor resource management with cooperative sensors for preventive vehicle safety applications," in *Proc. Workshop Sensor Data Fusion: Trends, Solutions, Appl.*, 2013, pp. 1–6.
[31] F. Johansson and G. Falkman, "Real-time allocation of defensive resources to rockets, artillery, and mortars," in *Proc. Int. Conf. Inf. Fusion*, 2010, pp. 1–8. [Online]. Available: http://ieeexplore.ieee.org/xpl/articleDetails.jsp?arnumber=5712026
[32] D. Papageorgiou and M. Raykin, "A risk-based approach to sensor resource management," in *Advances in Cooperative Control and Optimization*, vol. 369. Berlin. Germany: Springer, 2007, pp. 129–144.
[33] M. Ditzel, L. Kester, S. van den Broek, and M. van Rijn, "Cross-layer utility-based system optimization," in *Proc. Int. Conf. Inf. Fusion*, 2013, pp. 507–514. [Online]. Available: http://ieeexplore.ieee.org/xpl/articleDetails.jsp?arnumber=6641322
[34] T. de Groot, O. Krasnov, and A. Yarovoy, "Mission-driven sensor management based on expected-utility and prospect objectives," in *Proc. Int. Conf. Inf. Fusion*, 2014, pp. 1–8. [Online]. Available: http://ieeexplore.ieee.org/xpl/articleDetails.jsp?arnumber=6916123
[35] T. de Groot, O. Krasnov, and A. Yarovoy, "Mission-driven resource allocation based on subjective input with extra level of uncertainty," in *Proc. Int. Conf. Inf. Fusion*, 2014, pp. 1–7. [Online]. Available: http://ieeexplore.ieee.org/xpl/articleDetails.jsp?arnumber=6916124
[36] M. Friedman and L. J. Savage, "The utility analysis of choices involving risk," *J. Political Economy*, vol. 56, no. 4, pp. 279–304, 1948. [Online]. Available: http://www.jstor.org/stable/1826045
[37] P. J. Schoemaker, "The expected utility model: Its variants, purposes, evidence and limitations," *J. Econom. Lit.*, vol. 20, no. 2, pp. 529–563, 1982. [Online]. Available: http://www.jstor.org/stable/2724488
[38] A. N. Steinberg, "Foundations of situation and threat assessment," in *Handbook of Multi sensor Data Fusion*. Boca Raton, FL, USA: CRC Press, 2008, pp. 437–501.
[39] J. Beaver, R. Kerekes, and J. Treadwell, "An information fusion framework for threat assessment," in *Proc. Int. Conf. Inf. Fusion*, 2009, pp. 1903–1910.
[40] M. Barlow, A. Yang, and H. Abbass, "A temporal risk assessment framework for planning a future force structure," in *Proc. IEEE Symp. Comput. Intell. Security Defense Appl.*, 2007, pp. 100–107.
[41] B. R. Mahafza, *Radar Systems Analysis and Design Using MATLAB*. Boca Raton, FL, USA: Chapman & Hall, 2000.
[42] G. R. Curry, *Radar System Performance Modeling*. Norwood, MA, USA: Artech House, 2005.
[43] J. G. Proakis, *Digital Communications*. New York, NY, USA: McGraw-Hill, 1995.
[44] T. S. Rappaport, *Wireless Communications: Principles and Practice*. Upper Saddle River, NJ, USA: Prentice-Hall, 1996.
[45] S. Lin and D. J. Costello, *Error Control Coding*, 2nd ed. Englewood Cliffs, NJ, USA: Prentice-Hall, 2004.
[46] A. A. Markov, "Extension of the limit theorems of probability theory to a sum of variables connected in a chain," in *Dynamic Probabilistic Systems (Volume 1: Markov Chains)*. New York, NY, USA: Wiley, 1971, pp. 552–577.
[47] S. Dasgupta, C. Papadimitriou, and U. Vazirani, *Algorithms*. New York, NY, USA: McGraw-Hill, 2006.
[48] S. J. Julier and J. K. Uhlmann, "Consistent debiased method for converting between polar and Cartesian coordinate systems," *Proc. SPIE*, vol. 3086, pp. 110–121, 1997.
[49] E. Ruzanski, V. Chandrasekar, and Y. Wang, "The CASA nowcasting system," *J. Atmospheric Ocean. Technol.*, vol. 28, no. 5, pp. 640–655, 2011.
[50] S. E. Pilnick and J. Landa, "Airborne radar search for diesel submarines," DTIC Doc., Tech. Rep. 444346, 2005.
[51] R. H. Vollmerhausen, E. Jacobs, and R. G. Driggers, "New metric for predicting target acquisition performance," *Opt. Eng.*, vol. 43, no. 11, pp. 2806–2818, 2004.

Teun H. de Groot was born in Voorburg, The Netherlands. He received the B.Sc. and M.Sc. degrees in electrical engineering *(cum laude)* and Ph.D. degree from the Delft University of Technology, Delft, The Netherlands, in 2008, 2010, and 2015, respectively.

His graduation project was about acoustic sensor networks and was conducted at Thales Netherlands. During his Ph.D., he was with the Microwave Sensing, Signals and Systems research group, Delft University of Technology and worked on resource management for reconfigurable sensors as part of the Sensor Technology Applied in Reconfigurable Systems project.

Oleg A. Krasnov received the M.S. degree in radio physics from Voronezh State University, Voronezh, Russia, in 1982, and the Ph.D. degree in radiotechnique from the National Aerospace University "Kharkov Aviation Institute," Kharkiv, Ukraine, in 1994.

In 1999, he joined the International Research Center for Telecommunications and Radar, Delft University of Technology, Delft, The Netherlands. Since 2009, he has been a Senior Researcher with the Faculty of Electrical Engineering, Mathematics, and Computer Science, Microwave Sensing, Signals and Systems (MS3) section, Delft University of Technology, and become an Universitair Docent (Assistant Professor) in 2012. His research interests include radar waveforms, signal and data processing algorithms for polarimetric radars and distributed radar systems, multisensor atmospheric remote sensing, optimal resource management of adaptive radar sensors, and distributed systems.

Dr. Krasnov served as the Secretary of the 9th European Radar Conference, Amsterdam, The Netherlands.

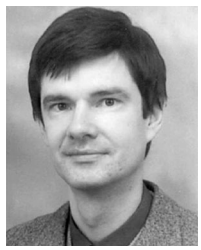

Alexander G. Yarovoy (M'95–SM'04–F'15) received the Diploma degree (with honors) in radiophysics and electronics and the Candidate Phys. & Math. Sci. and Doctor Phys. & Math. Sci. degrees in radiophysics from Kharkov State University, Kharkiv, Ukraine, in 1984, 1987, and 1994, respectively.

In 1987, he joined the Department of Radiophysics, Kharkov State University as a Researcher and became a Professor in 1997. From September 1994 to 1996, he was with the Technical University of Ilmenau, Ilmenau, Germany as a Visiting Researcher. Since 1999, he has been with the Delft University of Technology, Delft, The Netherlands. Since 2009 he leads there as a Chair of Microwave Sensing, Systems and Signals. His main research interests include ultra-wideband microwave technology and its applications (in particular, radars) and applied electromagnetics (in particular, UWB antennas). He has authored or coauthored more than 250 scientific or technical papers and 14 book chapters. He holds four patents.

Prof. Yarovoy served as a Guest Editor of five special issues in IEEE TRANSACTIONS and other journals.